LBL-29340
Preprint

Lawrence Berkeley Laboratory
UNIVERSITY OF CALIFORNIA

Materials & Chemical Sciences Division

Submitted to Physical Review Letters

Far Infrared Conductivity of TaS_3: Identification of the Intrinsic Charge Density Wave Excitation Modes

W.N. Creager, P.L. Richards, and A. Zettl

July 1990

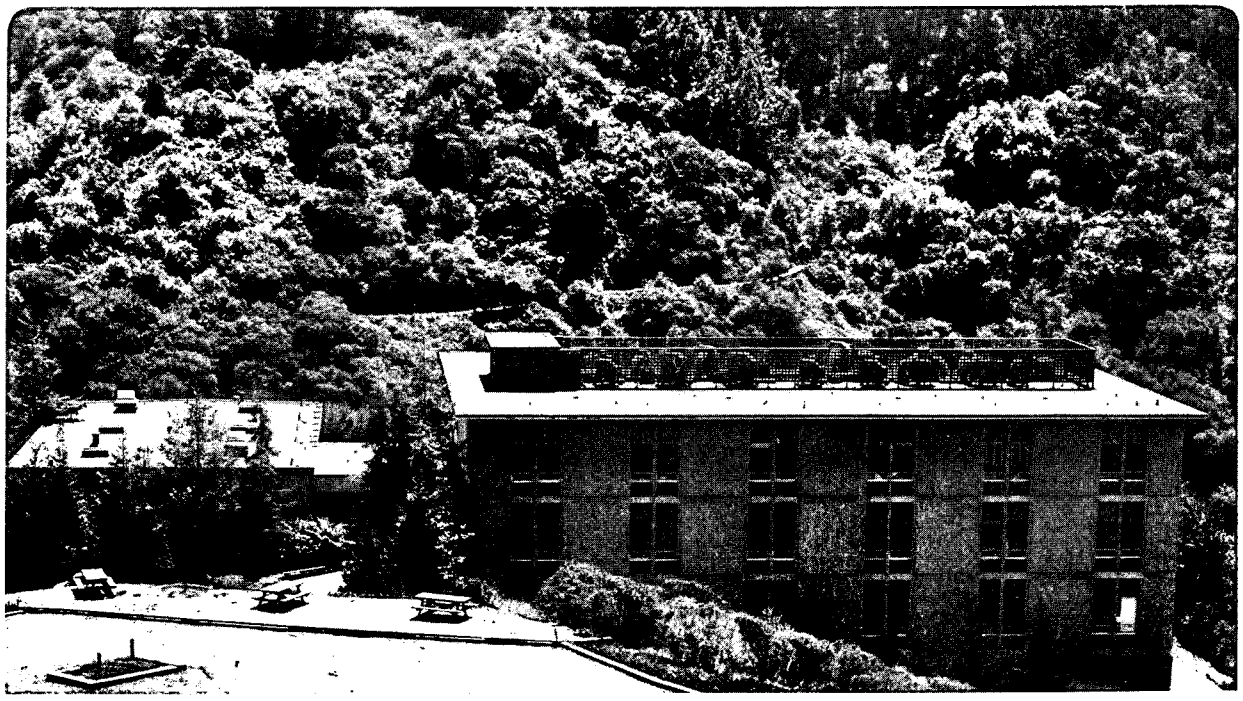

LOAN COPY
Circulates
for 2 weeks
Bldg. 50 Library.
LBL-29340
Copy 2

Prepared for the U.S. Department of Energy under Contract Number DE-AC03-76SF00098.

DISCLAIMER

This document was prepared as an account of work sponsored by the United States Government. While this document is believed to contain correct information, neither the United States Government nor any agency thereof, nor the Regents of the University of California, nor any of their employees, makes any warranty, express or implied, or assumes any legal responsibility for the accuracy, completeness, or usefulness of any information, apparatus, product, or process disclosed, or represents that its use would not infringe privately owned rights. Reference herein to any specific commercial product, process, or service by its trade name, trademark, manufacturer, or otherwise, does not necessarily constitute or imply its endorsement, recommendation, or favoring by the United States Government or any agency thereof, or the Regents of the University of California. The views and opinions of authors expressed herein do not necessarily state or reflect those of the United States Government or any agency thereof or the Regents of the University of California.

LBL-29340

Far Infrared Conductivity of TaS_3: Identification of the Intrinsic Charge Density Wave Excitation Modes

W.N. Creager, P.L. Richards, and A. Zettl

Department of Physics
University of California

and

Materials and Chemical Sciences Division
Lawrence Berkeley Laboratory
University of California
Berkeley, CA 94720

This work was supported in part by the National Science Foundation Grant No. DMR 84-00041, by the Director, Office of Energy Research, Office of Basic Energy Science, Materials Sciences Division of the U.S. Department of Energy under Contract No. DE-AC03-76SF00098, and by additional support to WNC from the IBM Pre-doctoral Fellowship Program.

Far Infrared Conductivity of TaS_3: Identification of the Intrinsic Charge Density Wave Excitation Modes

W.N. Creager, P.L. Richards, and A. Zettl

Department of Physics, University of California at Berkeley, and Materials and Chemical Sciences Division of the Lawrence Berkeley Laboratory, Berkeley, California 94720

(Received

The far infrared (FIR) reflectance of the charge density wave (CDW) conductor TaS_3 has been measured from 3 to 700cm^{-1}, over the temperature range from 15K to 300K. For incident radiation polarized parallel to the long axis of the crystals, a strong reflection edge correlated with the formation of the CDW appears near 80cm^{-1}. The associated conductivity shows no dramatic conduction mode in the FIR. These results, which are in sharp contrast to the observed behavior in the related CDW materials $(TaSe_4)_2I$ and $K_{0.3}MoO_3$, rule out models of a "generic FIR mode" in CDW excitations.

PACS# 71.45.Lr; 72.15.Nj; 78.30.Hv

One of the most outstanding features of relatively weakly pinned charge density wave (CDW) conductors is the unusual ac response spectrum. It is well established that there are at least three distinct and clearly-defined excitation modes: dielectric relaxation (at audio frequencies), the pinned acoustic phason (in the microwave region), and single particle excitations across the Peierls gap (at frequencies near 10^{13}-10^{14}Hz).[1]

A recent far-infrared (FIR) study[2] demonstrated that, in addition to the three established excitation modes, the CDW conductor $(TaSe_4)_2I$ has a giant conductivity mode in the FIR frequency range between the acoustic phason and the Peierls gap. Reinterpretation[2] of several previously published conductivity data sets on the blue bronze $K_{0.3}MoO_3$ shows that this CDW conductor most probably also has a distinct giant FIR mode. Hence, a very prominent fourth IR-active mode exists in the two CDW materials for which the full ac response spectrum is known.

It has been suggested that the giant FIR mode observed in $(TaSe_4)_2I$ and $K_{0.3}MoO_3$ may be generic to all CDW conductors and, on this basis, several general CDW conductivity models have been constructed. On the other hand, both $(TaSe_4)_2I$ and $K_{0.3}MoO_3$ are relatively complicated CDW systems (as discussed below), and it is possible that the giant FIR mode arises from peculiarities of the materials.

We report on FIR reflectivity measurements of the CDW conductor TaS_3 which, together with previous microwave[3,4] and

optical[5,6] measurements, complete the excitation spectrum for this system. Despite a rather complicated FIR reflectance in the CDW state, we show conclusively that no giant FIR mode exists in TaS_3. This rules out models which predict a generic FIR CDW excitation mode. Subtle but important differences between the CDW structures of TaS_3 and $(TaSe_4)_2I$ (and $K_{0.3}MoO_3$) allow us to infer the origin of the previously unidentified giant FIR mode.

High-purity crystals of TaS_3 were grown by conventional vapor transport methods. In order to prepare a sample suitable for FIR reflectance studies, several thousand single crystals were aligned by hand into an opaque mat 1cm in diameter. The crystals in the mat were held in place by a trace amount of a plastic resin.[7] An independent check of the resin alone showed it to have no strong modes in the FIR frequency range and no spectral features in common with those measured for the crystal mat. The sample temperature could be varied from 15K to 300K using a continuous-flow He refrigerator. Polarized light from a Michelson Fourier Transform interferometer illuminated the sample, and the reflected light was detected by a composite bolometer[8] operated at 1.5K. During a run the sample could be replaced by a polished brass surface for normalization purposes. Reflectance measurements were made at numerous temperatures both above and below the CDW transition temperature Tp=220K, with light polarized parallel and perpendicular to the chain

axis. We here report only on measurements with light polarized parallel to the chain (long) axis of the crystal.

Fig. 1 shows the measured FIR reflectance of TaS_3 on a logarithmic frequency scale, for two representative temperatures. The dashed line is the room temperature reflectance, which decreases smoothly from approximately 92% below $25cm^{-1}$ to approximately 8% at $700cm^{-1}$. The solid line is the reflectance at 13K, in the CDW state well below T_p. The low temperature reflectance falls, with oscillations, from 97% at $3cm^{-1}$ to 90% at $9cm^{-1}$, and then rises again to 96% at $20cm^{-1}$. A gradual drop in the reflectance begins at about $40cm^{-1}$, culminating in a sharp fall from about 75% at $60cm^{-1}$ to about 6% at $76cm^{-1}$. This dramatic reflection edge near $70cm^{-1}$ begins to develop at about 200K, just below T_p, and it sharpens continuously as the temperature is lowered. Beyond the reflectance edge, there is a series of narrow peaks in the reflectance at 83, 89, and $92cm^{-1}$ followed by a broad maximum centered at $150cm^{-1}$. The reflectance stabilizes to about 9% at $300cm^{-1}$ and remains featureless and flat out to $700cm^{-1}$. We note the absence of any outstanding feature near $500cm^{-1}$ that might be associated with the $500cm^{-1}$ anomaly[6] observed in transverse-polarized bolometric absorption spectra of TaS_3.

The complex dielectric function, $\varepsilon(\omega)$, is most directly obtained from the reflectance via a Kramers-Kronig calculation, for which it is desirable to have reflectance data over as wide a frequency range as possible. For this

purpose we have generated effective reflectance data for frequencies below our experimental limit of $3cm^{-1}$ by converting microwave conductivity data previously measured[3] on TaS_3 to reflectance. These microwave data points are shown as triangles in Fig. 1; they agree well with the trend of the measured reflectance at low frequencies.[9] The Peierls gap[5] is expected to affect the reflectance near $1200cm^{-1}$. Modelling of this feature was found to have little effect on the dielectric function calculated at lower frequencies, so the high frequency reflectance was simply continued at its $700cm^{-1}$ value.

Fig. 2 shows the dielectric function $\varepsilon(\omega)$ for TaS_3 calculated from the 13K reflectance curve of Fig. 1. The dashed and solid lines are the real part ε_1 and the imaginary part ε_2, respectively. The vertical scale has been expanded above $50cm^{-1}$ to show detailed structure at high frequencies. The inset shows the low frequency behavior of $\varepsilon(\omega)$ more clearly. Fig. 2 shows that ε_1 crosses from its large positive value at zero frequency to negative values at about $1cm^{-1}$, reflecting the pinned acoustic phason mode near this frequency. At higher frequencies, ε_1 then recovers and slowly climbs to another zero crossing near $70cm^{-1}$ that corresponds to the dramatic infrared reflectance edge between 70 and $80cm^{-1}$.

Aside from the dominant phason mode observed near $1cm^{-1}$ in Fig. 2, there are several other identifiable modes that modify the gradual rise in ε_1 and affect the location of the

zero crossing. To determine the relative strengths of these smaller modes, we fit them to independent oscillators. The largest FIR mode in TaS_3 is marked by an arrow in Fig. 2. It has an oscillator strength $\Omega_p^2 \leq 6.2 \times 10^{26}$ at $10.6 cm^{-1}$ which is a factor of 40 smaller than the oscillator strength of the giant FIR mode[2] in $(TaSe_4)_2I$ at $38 cm^{-1}$. We conclude that no giant FIR mode exists in TaS_3. The reflectance edge in TaS_3 is a result of a zero crossing of the real part of the dielectric function, but that zero crossing is a manifestation of the microwave pinned acoustic phason mode rather than any single mode at infrared frequencies.

Our FIR measurements on TaS_3 essentially complete the excitation spectrum for this material. In Fig. 3, a comparison is made between the real part of the ac conductivity $\sigma(\omega)$ of TaS_3 and that of $(TaSe_4)_2I$ over a wide frequency range. Fig. 3a shows $\sigma(\omega)$ for TaS_3. The solid line is the FIR conductivity determined from this study; curves at lower[3] and higher[5] frequencies have been adapted from data published previously by other groups. Although not shown in Fig. 3a, the Kramers-Kronig analysis shows that the FIR conductivity determined in this study increases sharply just below 10^{11}Hz, in qualitative agreement with the microwave data. The pinned acoustic phason and the Peierls gap are labeled in the Figure. The data for the Peierls gap for TaS_3 are only schematic, since it is difficult to convert the published bolometric absorption spectrum[5] into an absolute conductivity. Dielectric relaxation occurs at

frequencies below those shown in the Figure. Fig. 3b shows a similar plot of $\sigma(\omega)$ for the related CDW conductor $(TaSe_4)_2I$, obtained from the literature.[2,10,11] The intrinsic conductivity modes are identified in the Figure, along with the giant FIR mode at approximately 10^{12}Hz. Comparing Figs. 3a and 3b dramatically shows the difference between the excitation spectra of these two similar CDW materials. The giant FIR mode is not a generic feature of CDW conductors.

We now discuss the implications of these results for general models of CDW conduction. At least two explanations of the giant FIR mode in $(TaSe_4)_2I$ suggest that a similar mode should be found in TaS_3 and in fact universally in CDW conductors. Sherwin et al.[2] considered an "optical phason" argument which draws an analogy between the optical phonon in ionic crystals like NaCl and a possible optically active mode in CDW materials that may arise from counter-oscillating regions of the CDW condensate with opposite relative charges. This idea is similar to the "first harmonic phason" described earlier by Walker.[12] Because this mode depends only on the presence of a CDW and not on the crystal structure, it should be a generic feature of CDW materials. Lyons and Tucker[13] have attributed the giant FIR mode to coherent oscillations of the CDW phase in tiny regions surrounding impurities. Again, this explanation assumes that an infrared conductivity resonance is a generic feature of CDW materials which are not perfectly pure. These mechanisms clearly do not generate a

large FIR oscillator strength in TaS_3 and are thus unlikely explanations for the giant mode seen in other CDW materials.

The absence of a giant resonance in TaS_3 suggests that there are only three intrinsic excitation modes in CDW conductors, and that the giant FIR mode in $(TaSe_4)_2I$ and $K_{0.3}MoO_3$ arises from peculiar properties of those materials. This finding give strong support to a model in which the giant mode arises through zone-folding,[2,14] which is sensitive to the relation of the Fermi surface to the Brillouin zone edge. Both $(TaSe_4)_2I$ and the blue bronze have $2k_F>\pi/a$, while TaS_3 is in a simpler class of materials with $2k_F<\pi/a$.

Mode generation through zone-folding was originally considered by Sugai, Sato, and Kurihara in their studies[14,15] of the Raman modes in $(TaSe_4)_2I$. In that material, the soft Kohn anomaly phonon is located near the edge of the second Brillouin zone. When the phonon dispersion curve is folded in the reduced zone scheme, the soft mode lies on a transverse optical branch above the transverse acoustic branch. As the temperature is decreased toward T_p, the TO Kohn anomaly begins to soften and triggers the CDW distortion in the usual way, but the interaction between the TO branch and the lower energy TA branch forces the TA branch to $\omega=0$ first. (Additionally, the degenerate modes at $q=\pm 2k_F$ are mixed to yield both a Raman and an infrared active mode for each branch.) In these materials the observed modes are understood as follows: the pinned acoustic phason mode seen

at microwave frequencies arises from the TA anomoly, the giant FIR mode from the TO Kohn anomaly, and the two small higher frequency modes from two more TO branches also produced by the folding of the original dispersion curve.

A situation analogous to that just described for $(TaSe_4)_2I$ could occur in any CDW material with $2k_F>\pi/a$ (such as $K_{0.3}MoO_3$), but not in TaS_3, where the Kohn anomaly is inside the Brillouin zone and is thus always on the lowest lying branch. Our interpretation suggests that a giant FIR excitation mode should be absent in other CDW materials with $2k_F<\pi/a$, such as $NbSe_3$, but may be present in KCP,[16] to which a zone-folding mode generation argument applies.

We thank Brian Burk for assistance in growing the TaS_3 crystals, and acknowledge helpful discussions with David Miller, Mark Sherwin, and Steve Donovan. This work is supported in part by NSF Grant No. DMR 84-00041 and by the Director, Office of Energy Research, Office of Basic Energy Science, Materials Sciences Division of the U.S. Department of Energy under Contract No. DE-AC03-76SF00098. W.N.C. acknowledges additional support from the IBM Pre-doctoral Fellowship Program.

References

[1]Charge Density Waves in Solids, edited by L.P. Gor'kov and G. Grüner (North-Holland, Amsterdam, 1989).

[2]M.S. Sherwin, A. Zettl, and P.L. Richards, Phys. Rev. **B 36**, 6708 (1987).

[3]S. Sridhar, D. Reagor, and G. Grüner, Phys. Rev. **B 34**, 2223 (1986).

[4]Wei-yu Wu, L. Mihály, George Mozurkewich and G. Grüner, Phys. Rev. Lett. **52**, 2382 (1984); S. Sridhar, D. Reagor, and G. Grüner, Phys. Rev. Lett. **55**, 1196 (1985).

[5]S. L. Herr, G. Minton, and J.W. Brill, Phys. Rev. **B 33**, 8851 (1986).

[6]G. Minton and J.W. Brill, Solid State Comm. **65**, 1069 (1988).

[7]Castin' craft clear casting resin, ETI, Fields Landing, CA 95537.

[8]A.E. Lange, E. Kreysa, S.E. McBride, P.L. Richards, and E.E. Haller, Int. J. IR + MM Waves **4**, 689 (1983).

[9]The reflectance oscillations in the 13K data between 3 and 9 cm^{-1} are approximately temperature independent and their spacing varies inversely with sample thickness. The true reflectance of an ideal semi-infinite sample would lie somewhere between the extrema of these Fabry-Perot oscillations. A line drawn smoothly through the middle of the oscillations agrees well with the reflectance derived from the microwave conductivity, and we used such smoothing in generating the dielectric constant discussed below.

Kramers-Kronig transforms performed with and without such smoothing indicate that smoothing the oscillations has no effect on the dielectric constant calculated above 12 cm^{-1}.

[10]Tae Wan Kim, D. Reagor, G. Grüner, K. Maki, and A. Virosztek, Phys. Rev. **B 40**, 5372 (1989).

[11]H.P. Geserich, G. Scheiber, M. Dürrler, F. Lévy, and P. Monceau, Physica **143B**, 198 (1986).

[12]M.B. Walker, Can. J. Phys. **56**, 127 (1978).

[13]W.G. Lyons and J.R. Tucker, Phys. Rev. **B 40**, 1720 (1989).

[14]S. Sugai, M. Sato, S. Kurihara, Phys. Rev. **B 32**, 6809 (1985).

[15]Shunji Sugai, Susumu Kurihara, and Masotoshi Sato, Physica **143B**, 195 (1986).

[16]R. Comès, M. Lambert, H. Launois, and H.R. Zeller, Phys. Rev. **B 8**, 571 (1973); B. Renker, H. Rietschel, L. Pintschovius, W. Gläser, P. Brüesch, D. Kuse, and M.J. Rice, Phys. Rev. Lett. **30**, 1144 (1973).

Figure Captions

1. Reflectance versus frequency for TaS_3 at 15K and 295K. The triangles are reflectances calculated from microwave frequency conductivities measured at 30 K in Reference 3.

2. The real part (dashed line) and imaginary part (solid line) of the dielectric function deduced by a Kramers-Kronig analysis of the 15K reflectivity data for TaS_3. Above 50 cm-1, the scales are expanded by a factor of 10.

3. a) Real part of the conductivity versus frequency for TaS_3. The solid line is this work, the squares (connected by a line to guide the eye) represent microwave measurements at 30 K from Ref. 8, and the dashed line schematically represents the Peierls gap from Ref. 7. b) Real part of the conductivity versus frequency for $(TaSe_4)_2I$ from the literature. The squares (connected by a line to guide the eye) represent microwave measurements at 50K from Ref 10, the solid line is calculated from the FIR oscillators reported in Ref. 2, and the triangles represent the conductivity near the Peierls gap measured at 140 K in Ref. 11.

Fig 1

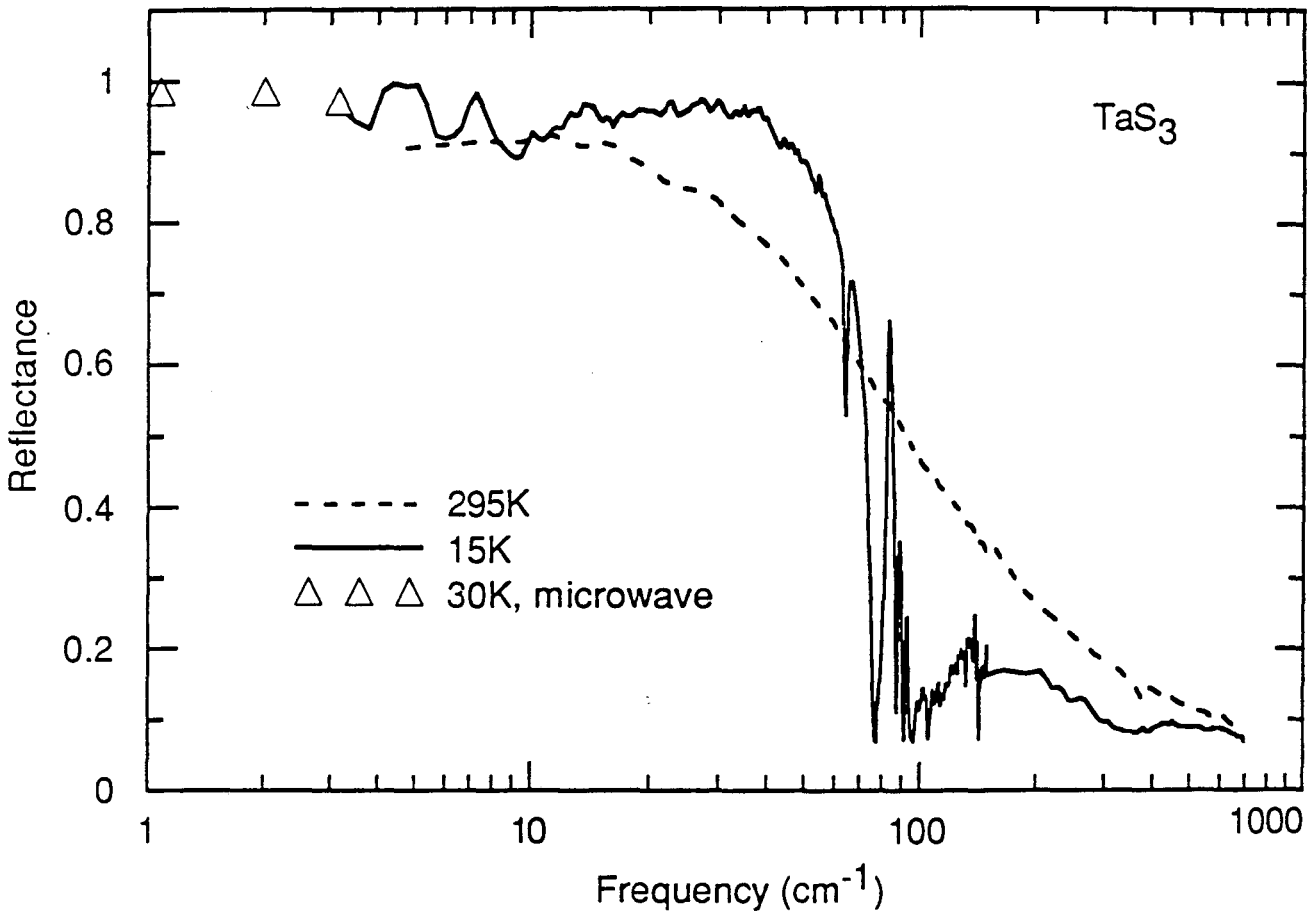

Figure 1

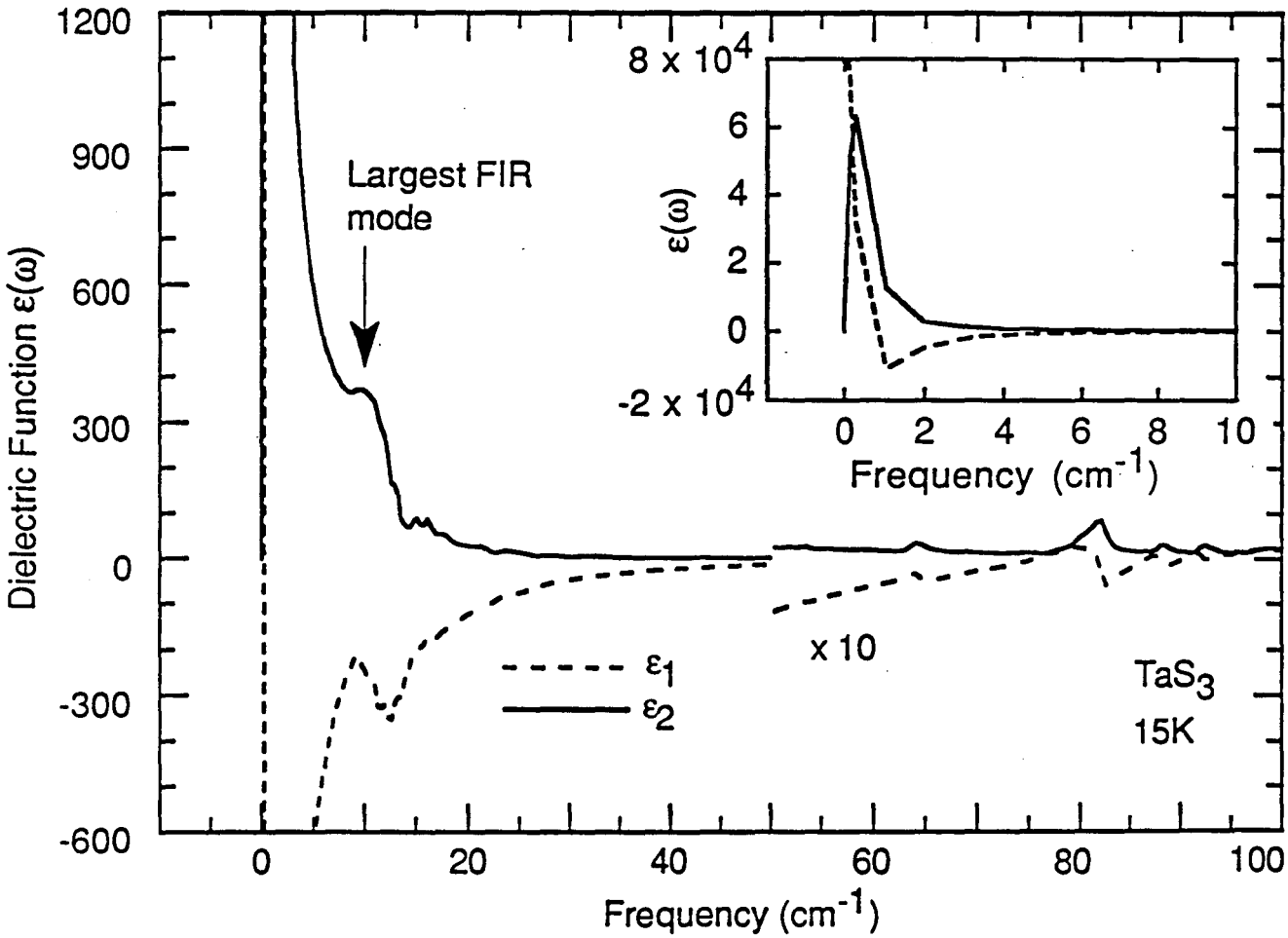
1200
900
600
300
0
-300
-600
Dielectric Function ε(ω)
Largest FIR
mode
8 x 10^4
6
4
2
0
-2 x 10^4
ε(ω)
0
2
4
6
8
10
Frequency (cm^-1)
x 10
ε1
ε2
TaS3
15K
0
20
40
60
80
100
Frequency (cm^-1)

Figure 2

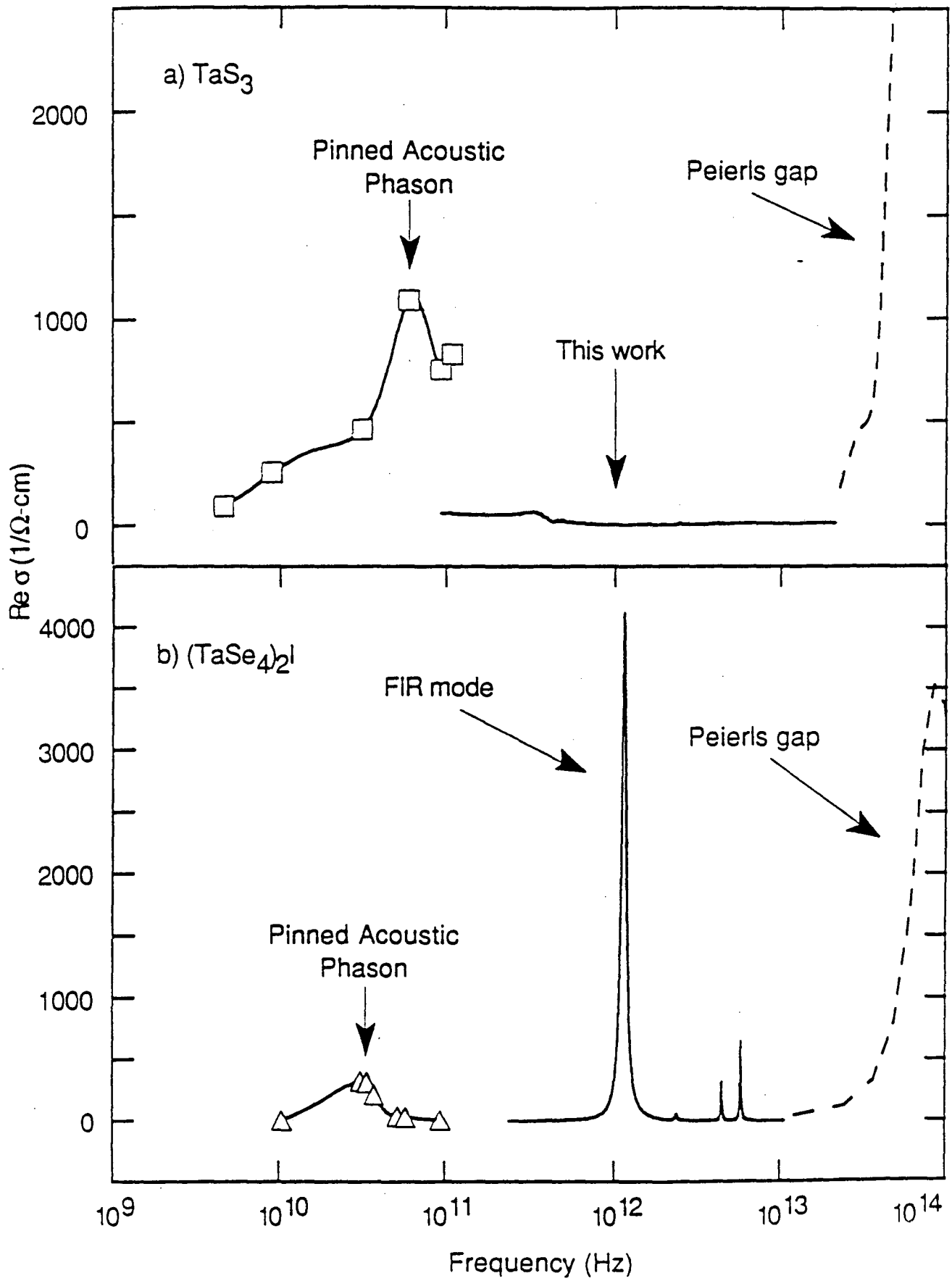
a) TaS3
2000
1000
0
Pinned Acoustic
Phason
Peierls gap
This work
Re σ (1/Ω-cm)
b) (TaSe4)2I
4000
3000
2000
1000
0
FIR mode
Peierls gap
Pinned Acoustic
Phason
10^9
10^10
10^11
10^12
10^13
10^14
Frequency (Hz)

Figure 3

LAWRENCE BERKELEY LABORATORY
UNIVERSITY OF CALIFORNIA
INFORMATION RESOURCES DEPARTMENT
BERKELEY, CALIFORNIA 94720